Inelastic and Stability Analysis of Linearly Tapered Box Columns under Biaxial Bending and Torsion

by

Minoru SHUGYO*, Jian Ping LI**
and Nobuo OKA***

The inelastic instability of cantilever columns with tapered square hollow section under the combined action of axial force, biaxial bending and torsion is studied. A new elastic–plastic tangent stiffness matrix for members with closed thin walled section is used to investigate the behavior. The stiffness matrix uses a tangent coefficient matrix obtained by the numerical integration of the hardening moduli of the fibers about the member section to calculate the generalized plastic strain increments. The effect of torsion is considered in the fiber level using von Mises yield criterion. The ultimate strength of the columns is obtained by using extended Horne's stability criterion, and the results are presented in the form of interaction diagrams.

1 INTRODUCTION

Tapered members have immense advantage when they are used as a corner columns in a space building frame[1, 2] . Richard Liew and Shanmugam[2] investigated the stability of tapered and symmetric pin–ended square box columns under the combined action of axial force and biaxial moments, and clarified that the taper slope has significant influence on the behavior and strength of these columns. However, the effect of torsional moment was ignored in the analyses, while a large torsional moment can arise by a small torsional deformation in the member with closed thin–walled section. Some factors which cause structure and member to twist are in a space building frame, e.g., eccentricity of the gravitational center, therefore, it is desirable to clarify the influence of torsional moment on the inelastic behavior of tapered square box columns.

In this paper the behavior of linearly tapered cantilever columns with square hollow section that collapse in elastic–plastic region is investigated. The column is subjected to biaxial bending in addition to constant axial force and torsion. The effect of torsion is considered in the fiber level using von Mises yield criterion. Parameters in the analysis are taper slope and amounts of axial thrust and torsion.

2 TAPERED COLUMNS

Figure 1 shows a tapered cantilever column considered herein. The column is linearly tapered along its length by varying the depth and width but keeping the cross section thickness constant. The taper slopes for the depth and width of the cross section along the length are assumed to be the same. The slope is defined as

$$\alpha=(D_0-D)/L \tag{1}$$

where D_0 and D are the depth of the cross section at the fixed and free end, respectively, and L is the length of the column.

Received on April 27, 1995
*Department of Structural Engineering
**Department of Structural Engineering
***Japan Steel Tower Co., Ltd.

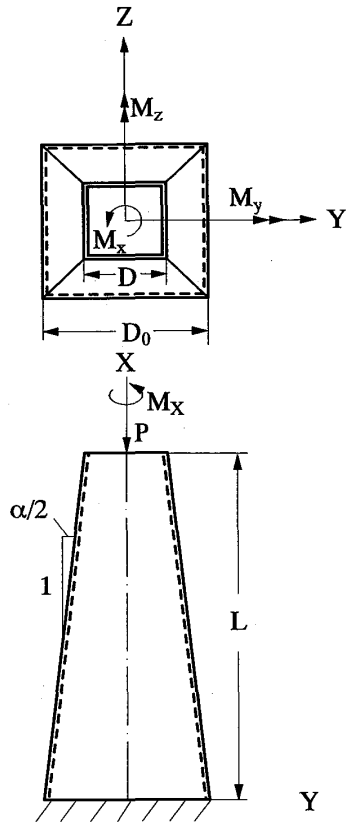

Fig. 1 Linearly tapered cantilever column

3 NUMERICAL METHOD

The numerical analysis is done by using a new method for geometrically and materially nonlinear analysis of steel member with uniform square hollow section. The method is an advanced finite element method. The column is divided into a number of elements along the length and it is assumed that each of these elements has a uniform cross section.

The relations between bending moment and displacement at the free end are obtained by step by step analysis, and the ultimate values of bending moments are determined by an extended Horne's stability criterion[2]

3.1 Geometrically nonlinear stiffness matrix

Member coordinate system (x,y,z) are shown in Fig. 2. The strain-displacement relationship adopted here is

$$\left.\begin{aligned}\varepsilon_x&=\frac{\partial u}{\partial x}+\frac{1}{2}\left(\frac{\partial v}{\partial x}\right)^2+\frac{1}{2}\left(\frac{\partial w}{\partial x}\right)^2\\ \gamma_{xy}&=\frac{\partial v}{\partial x}+\frac{\partial u}{\partial y}\\ \gamma_{xz}&=\frac{\partial w}{\partial x}+\frac{\partial u}{\partial z}\\ \varepsilon_y&=0\\ \varepsilon_z&=0\\ \gamma_{yz}&=0\end{aligned}\right\} \quad (2)$$

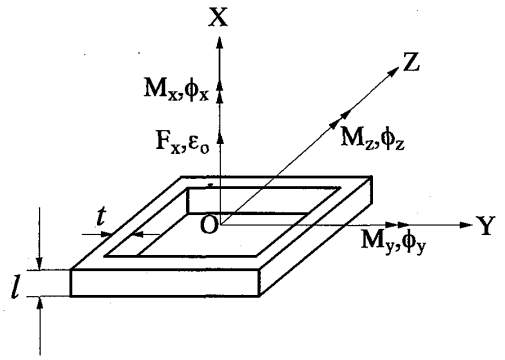

Fig. 2 Generalized stresses and strains of an element

where u, v, and w are the displacements of an arbitrary point in x-, y-, and z-direction, respectively. These values are related to the displacements u_0, v_0, and w_0, and the rotation angle ϕ_0 of the point on x-axis as

$$\left.\begin{aligned}u&=u_0-y\frac{dv_0}{dx}-z\frac{dw_0}{dx}\\ v&=v_0-z\phi_0\\ w&=w_0+y\phi_0\end{aligned}\right\} \quad (3)$$

Substituting Eq.(3) into Eq.(2) and utilizing an energy principle, we obtain the following equation:

$$d\boldsymbol{Q}=\boldsymbol{K}^e d\boldsymbol{q}^e \quad (4)$$

in which $\boldsymbol{K}^e$ is the geomertrically nonlinear tangent stiffness matrix and $\boldsymbol{Q}$ and $\boldsymbol{q}^e$ are nodal forces and elastic displacements of an element, respectively. $\boldsymbol{Q}$ and $\boldsymbol{q}^e$ have the following components[3] :

$$\left.\begin{aligned}\boldsymbol{Q}&=[F_{xi}\ F_{yi}\ F_{zi}\ M_{xi}\ M_{yi}\ M_{zi}\ F_{xj}\ F_{yj}\ F_{zj}\ M_{xj}\ M_{yj}\ M_{zj}]^T\\ \boldsymbol{q}^e&=[u_i^e\ v_i^e\ w_i^e\ \theta_{xi}^e\ \theta_{yi}^e\ \theta_{zi}^e\ u_j^e\ v_j^e\ w_j^e\ \theta_{xj}^e\ \theta_{yj}^e\ \theta_{zj}^e]^T\end{aligned}\right\} \quad (5)$$

where F_{kl} denotes the force in k-direction at node l; M_{kl} denotes the bending or torsional moment about k-axis at node l. Components of $\boldsymbol{q}^e$ are the corresponding elastic displacements. Cubic functions for v_0 and w_0 and linear functions for u_0 and ϕ_0 are adopted as displacement fields, and no higher order terms in $\boldsymbol{K}^e$ are neglected herein.

3.2 Plastic tangent coefficient matrix for a cross section

In the present method, plastic deformation increment is estimated utilizing tangent coefficient matrix for a cross section. The tangent coefficient matrix is obtained by numerical integration of tangent stiffnesses of fibers which compose the element.

3.2.1 Incremental stress-strain relationship of a fiber

Assuming that only axial stress and shear stress due to St. Venant torsion participate in yielding of a fiber, the von Mises yield condition can be written as follows:

$$f(\sigma_{ij})=\sigma^2+3\tau^2-\sigma_y^2=0 \tag{6}$$

where σ is a normal stress due to axial force and bending moments, τ is a shear stress due to St. Venant torsion, and σ_y is the yield stress of a fiber. Denoting the translation of the center of the yield surface by α_{ij}, the subsequent yield condition which behaves according to Ziegler's modified kinematic hardening rule[4] is represented as follows:

$$f(\sigma_{ij},\alpha_{ij})=0 \tag{7}$$

The flow rule is represented as

$$d\varepsilon_{ij}^p=\frac{\partial f(\sigma_{ij},\alpha_{ij})}{\partial\sigma_{ij}}d\lambda \tag{8}$$

where $d\varepsilon_{ij}^p$ is the increment of plastic strain, and $d\lambda$ is a positive scalar quantity. Introducing a parameter c which characterizes the hardening behavior of the material, $d\lambda$ is obtained here as

$$d\lambda=\frac{m_1d\sigma+m_2d\tau}{2a} \tag{9}$$

where

$$a=c(m_1^2+m_2^2),\quad m_1=\sigma-\xi,\quad m_2=3(\tau-\eta) \tag{10}$$

and ξ and η are the translations in σ-and τ-direction, respectively. The parameter c can be obtained by the following relationship using the tangent modulus H' of the uniaxial stress-plastic strain relationship of the material.

$$c=\frac{2}{3}H' \tag{11}$$

Substituting equation (9) into equation (8), we obtain the following equation:

$$\left.\begin{aligned} d\varepsilon^p&=\frac{m_1^2d\sigma+m_1m_2d\tau}{a}\\ d\gamma^p&=\frac{m_2m_1d\sigma+m_2^2d\tau}{a}\end{aligned}\right\} \tag{12}$$

Now, the elastic strain increments $d\varepsilon_{ij}^e$ are related to the stress increments $d\sigma_{ij}$ through Hooke's law,

$$\begin{Bmatrix}d\varepsilon^p\\ d\gamma^p\end{Bmatrix}=\begin{bmatrix}1/E & 0\\ 0 & 1/G\end{bmatrix}\begin{Bmatrix}d\sigma\\ d\gamma\end{Bmatrix} \tag{13}$$

where E and G are Young's and shear moduli, respectively. From equations (12) and (13) the incremental total stress-strain relation of a fiber is expressed as

$$\begin{Bmatrix}d\varepsilon\\ d\gamma\end{Bmatrix}=\left[\begin{bmatrix}1/E & 0\\ 0 & 1/G\end{bmatrix}+\frac{1}{a}\begin{bmatrix}m_1^2 & m_1m_2\\ m_2m_1 & m_2^2\end{bmatrix}\right]\begin{Bmatrix}d\sigma\\ d\gamma\end{Bmatrix} \tag{14}$$

and the inverse relationship can be obtained as

$$\begin{Bmatrix}d\sigma\\ d\gamma\end{Bmatrix}=\begin{bmatrix}D_{11} & D_{12}\\ D_{21} & D_{22}\end{bmatrix}\begin{Bmatrix}d\varepsilon\\ d\gamma\end{Bmatrix}\equiv\boldsymbol{D}^p\begin{Bmatrix}d\varepsilon\\ d\gamma\end{Bmatrix} \tag{15}$$

The increments of translation $d\alpha_{ij}$ is expressed as

$$d\alpha_{ij}=\{\sigma_{ij}-\alpha_{ij}\}d\mu \tag{16}$$

where $d\mu$, a positive scalar, can be determined from the condition that the total differential of the yield surface equals zero and is given here as follows:

$$d\mu=\frac{m_1d+m_2d\tau}{\sigma_y^2} \tag{17}$$

3.2.2 Plastic tangent coefficient matrix

The member coordinate system (x,y,z) and components of generalized stress vector $\boldsymbol{F}$ and generalized strain vector Δ are shown in Fig. 2. The components of $\boldsymbol{F}$ and Δ can be written as

$$\left.\begin{aligned}\boldsymbol{F}&=[F_x\ M_x\ M_y\ M_z\ ]^T\\ \Delta&=\ [\varepsilon_0\ \phi_x\ \phi_y\ \phi_z]^T\end{aligned}\right\} \tag{18}$$

where F_x is an axial force, M_x is a torsional moment, M_y and M_z are bending moments, and the components of Δ are corresponding generalized strains, respectively. The increments of generalized stresses are related to the stress increments by

$$\left.\begin{aligned}dF_x&=\int d\sigma dA\quad dM_x=\int d\tau hdA\\ dM_y&=\int d\sigma zA\quad dM_z=-\int d\sigma ydA\end{aligned}\right\} \tag{19}$$

while the strain increments are related to the increments of generalized strains by

$$\left.\begin{aligned}d\varepsilon&=d\varepsilon_0+zd\phi_y-yd\phi_z\\ d\gamma&=hd\phi_x\end{aligned}\right\} \tag{20}$$

where h is the distance from the centroid of the cross section to the center of the member wall. Substituting equations (15) and (20) into equation (19), we obtain the incremental generalized stress-generalized strain relationship:

$$dF=\begin{bmatrix} \int D_{11}dA & \int D_{12}hdA & \int D_{11}zdA & -\int D_{11}ydA \\ \int D_{21}hdA & \int D_{22}h^2dA & \int D_{21}hzdA & -\int D_{21}hydA \\ \int D_{11}zdA & \int D_{12}hzdA & \int D_{11}z^2dA & -\int D_{11}yzdA \\ -\int D_{11}ydA & -\int D_{12}hydA & -\int D_{11}yzdA & \int D_{11}y^2dA \end{bmatrix} d\Delta \equiv s\,d\Delta \quad (21)$$

where s is a tangent coefficient matrix. Let s^e denote an elastic tangent coefficient matrix and let $d\Delta^e$ and $d\Delta^p$ denote the elastic and plastic components of $d\Delta$, respectively, then

$$\left.\begin{aligned} dF&=s^e d\Delta^e \\ d\Delta&=d\Delta^e+d\Delta^p \end{aligned}\right\} \quad (22)$$

Substituting equation (21) into (22) yields

$$d\Delta^p=(s^{-1}-s^{e-1})\,dF\equiv s'\,dF \quad (23)$$

where s' is a plastic tangent coefficient matrix. The elastic tangent coefficient matrix s^e is constant for any state of the section. The components of the tangent coefficient matrix can be obtained by numerical integration. Figure 3 shows partitioning of a cross section used in the present analysis. The stress and the tangent stiffness in each fiber are obtained as the average values at its centroid. The "tangent stiffness method[5]" can be used to determine correctly the matrix s.

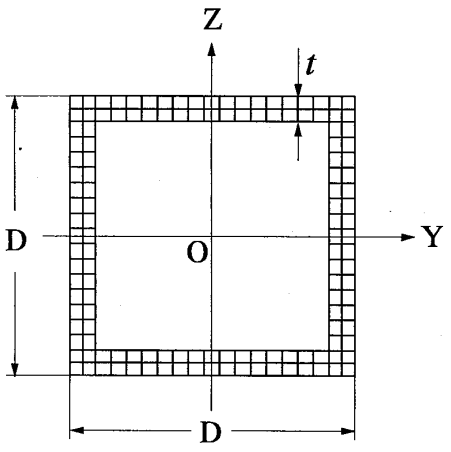

Fig. 3 Partitioning of a cross section

3.3 Elastic-plastic tangent stiffness matrix

The following assumptions are made concerning the mechaninal behavior of the yielded member: (1) Plastic deformations consist of only four components that correspond to axial force, biaxial bending moments, and torsional moment. (2) Each member has a uniform cross section and it does not distort. (3) An actual generalized plastic strain in a short member shown in Fig. 2 generally distributes as shown in Fig. 4 (a). It is idealized with generalized plastic strains distributing linearly with the values at the member ends i and j as shown in Fig.4 (b). (4) Incremental plastic deformations in the two $l/2$ portions occur concentrically at the member ends i and j, respectively, where l is the length of the member.

Now let us define plastic displacement increments dq_i^p, dq_j^p as

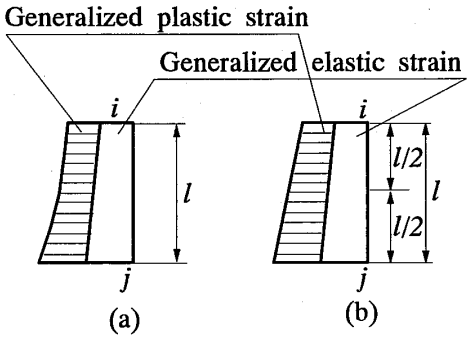

Fig. 4 Assumption of generalized plastic strain distribution in an element

$$\left.\begin{aligned} dq_i^p&=[du_i^p \;\; 0 \;\; 0 \;\; d\theta_{xi}^p \; d\theta_{yi}^p \; d\theta_{zi}^p]^T \\ dq_j^p&=[du_j^p \;\; 0 \;\; 0 \;\; d\theta_{xj}^p \; d\theta_{yj}^p \; d\theta_{zj}^p]^T \end{aligned}\right\} \quad (24)$$

which are the nodal displacement increments due to the generalized plastic strain increments of a member. These plastic displacement increments can be obtained as described below.

The generalized stresses at the member ends are obtained by the nodal forces with their coordinate transformation. Using these generalized stresses we can obtain the plastic tangent coefficient matrices s'_i and s'_j utilizing the procedure explained in the preceding section. Representing the components of s'_i by $(s'_{kl})_i$, a new square matrix s_i^p of 6 th order can be obtained as follows:

$$\boldsymbol{s}_i^p=\begin{bmatrix}(s'_{11})_i & 0 & 0 & (s'_{12})_i & (s'_{13})_i & (s'_{14})_i\\ 0 & 0 & 0 & 0 & 0 & 0\\ 0 & 0 & 0 & 0 & 0 & 0\\ (s'_{21})_i & 0 & 0 & (s'_{22})_i & (s'_{23})_i & (s'_{24})_i\\ (s'_{31})_i & 0 & 0 & (s'_{32})_i & (s'_{33})_i & (s'_{34})_i\\ (s'_{41})_i & 0 & 0 & (s'_{42})_i & (s'_{43})_i & (s'_{44})_i\end{bmatrix} \quad (25)$$

Another new matrix $\boldsymbol{s}_j^p$ which corresponds to $\boldsymbol{s}'_j$ can be obtained similarly. In case of uniaxial bending, the plastic curvature increment distributes as shown in Fig. 5 from assumption (3). Hence the plastic rotation increment at the member end i can be expressed as follows from assumption (4) :

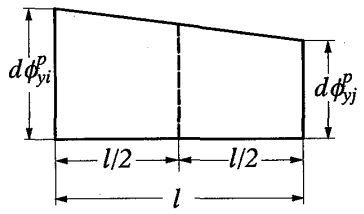

Fig. 5 Assumption of plastic curvature distribution in an element

$$-d\theta^p_{yi}=\frac{1}{2}\cdot\frac{l}{2}\left\{d\phi^p_{yi}+\frac{1}{2}(d\phi^p_{yi}+d\phi^p_{yj})\right\}=\frac{l}{2}\frac{3d\phi^p_{yi}+d\phi^p_{yj}}{4} \quad (26)$$

The plastic displacement increments at the member end i can be obtained by extending equation (26) considering the member coordinate system and expressed as

$$d\boldsymbol{q}_i^p=\frac{l}{2}\frac{3\boldsymbol{s}_i^p d\boldsymbol{Q}_i-\boldsymbol{s}_j^p d\boldsymbol{Q}_j}{4} \quad (27)$$

Similarly, for the member end j

$$d\boldsymbol{q}_j^p=\frac{l}{2}\frac{-\boldsymbol{s}_i^p d\boldsymbol{Q}_i+3\boldsymbol{s}_j^p d\boldsymbol{Q}_j}{4} \quad (28)$$

Rearranging equations (27) and (28) we obtain

$$\begin{Bmatrix}d\boldsymbol{q}_i^p\\ d\boldsymbol{q}_j^p\end{Bmatrix}=\frac{l}{8}\begin{bmatrix}3\boldsymbol{s}_i^p & -\boldsymbol{s}_j^p\\ -\boldsymbol{s}_i^p & 3\boldsymbol{s}_j^p\end{bmatrix}\begin{Bmatrix}d\boldsymbol{Q}_i\\ d\boldsymbol{Q}_j\end{Bmatrix}\equiv\boldsymbol{s}^p d\boldsymbol{Q} \quad (29)$$

Since the total displacement increments $d\boldsymbol{q}$ are the sum of the elastic components $d\boldsymbol{q}^e$ and the plastic components $d\boldsymbol{q}^p$, then

$$d\boldsymbol{q}^e=d\boldsymbol{q}-d\boldsymbol{q}^p \quad (30)$$

For the elastic components equation (4) is given, hence

$$d\boldsymbol{Q}=\boldsymbol{K}^e d\boldsymbol{q}-\boldsymbol{K}^e d\boldsymbol{q}^p \quad (31)$$

Substituting equation (29) into equation (31) we obtain

$$d\boldsymbol{Q}=\boldsymbol{K}^e d\boldsymbol{q}-\boldsymbol{K}^e\boldsymbol{s}^p d\boldsymbol{Q} \quad (32)$$

Rearranging equation (32) an elastic-plastic tangent stiffness matrix $\boldsymbol{K}^p$ is obtained as follows:

$$d\boldsymbol{Q}+\boldsymbol{R}=[I+\boldsymbol{K}^e\boldsymbol{s}^p]^{-1}\boldsymbol{K}^e d\boldsymbol{q}\equiv\boldsymbol{K}^p d\boldsymbol{q} \quad (33)$$

where $\boldsymbol{R}$ is the unbalanced force vector and $\boldsymbol{I}$ is the unit matrix.

The numerical analysis is carried out by a displacement controlled load increment method, using $\boldsymbol{K}^p$. Coordinate transformation matrix of a member is updated and rigid body displacements are separated in each step by using orientation matrix[6] .

4 NUMERICAL RESULTS

The proposed method was applied to the analysis of tapered cantilever box columns of varying proportions. Typical results for box columns of square cross sections having taper slopes, α, of 0.01 and-0.01 are presented in load-displacement curves in Figs. 6 and 7 . The columns were assumed to have sinusoidal initial deflections about both axes with maximum free end deflection of $L/500$. All results were obtained by assuming the D/t ratio at the free end as 40 and the nondimensionalized slenderness ratio λ as 0.4. λ was defined by the equation $\lambda=2L\sqrt{\varepsilon_y}/\pi r$, where ε_y is yield strain of material and r is radius of gyration about principal axis at the free end. The results in Figs. 6 and 7 show the relationships between bending moment and displacement at the free end. The effect of taper slopes on column strength is illustrated in Figs. 8-10 as the interaction diagrams for a column with $\lambda=0.4$. The ultimate strength of the column is obtained by using extended Horne's stability criterion[2] . Figure 8 is the comparison of the results of Richard Liew et al. and the present method. The results by two different method agree closely. Figures 9 and 10 show the effect of torsional moment on the ultimate strength of tapered columns under two values of axial force. It can be seen from the figures that the effect of torsional moment is significant in moment capacity of the column as the value of α decreases.

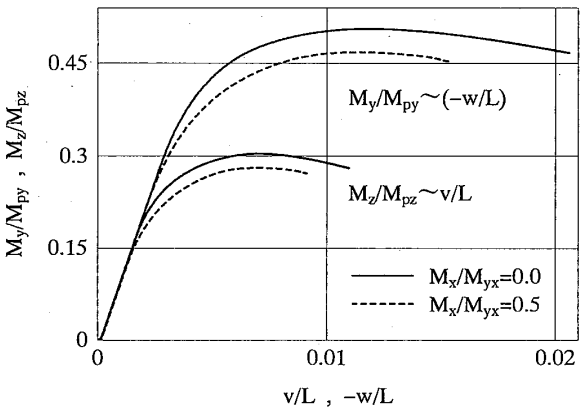

Fig. 6 Typical load-displacement curves for $\alpha=0.01$ $(P/P_y=0.5)$

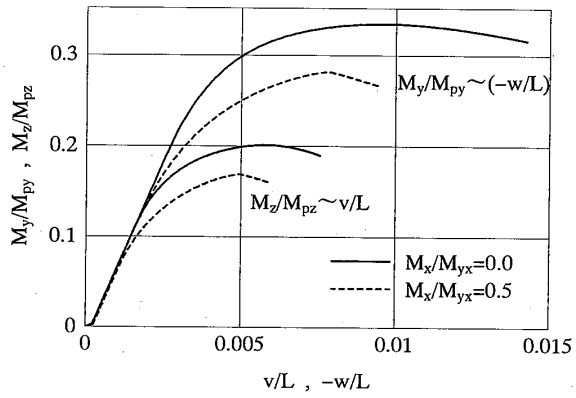

Fig. 7 Typical load-displacement curves for $\alpha=-0.01$ $(P/P_y=0.5)$

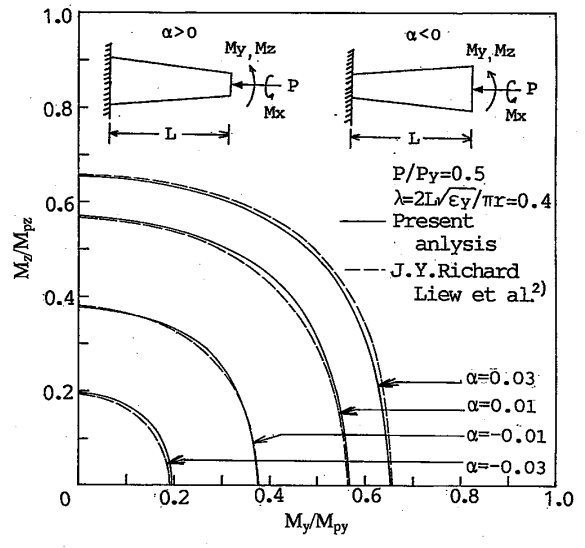

Fig. 8 Comparison of interaction curves for columms without torsion

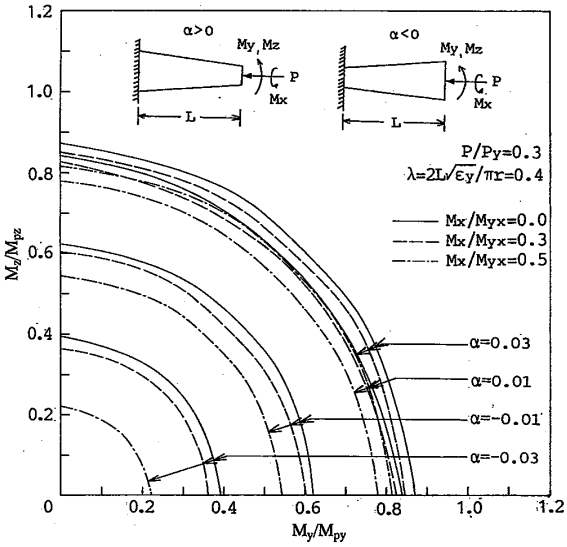

Fig. 9 Interaction curves for the collumms with $\lambda=0.4$ under $P/P_y=0.3$

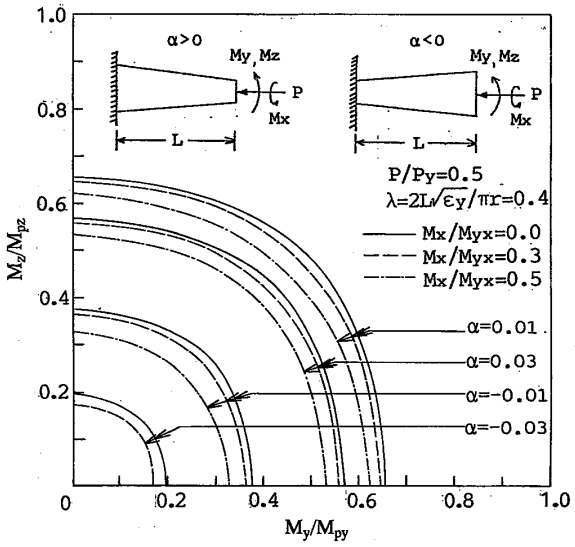

Fig. 10 Interaction curves for the collumms with $\lambda=0.4$ under $P/P_y=0.5$

5 CONCLUSIONS

A numerical method for elastic-plastic large deformation analysis of tapered box columns with square hollow section was presented and the inelastic instability of cantilever columns under the combined action of axial force, biaxial bending and torsion is studied. The results were given in the form of interaction diagrams and it becomes clear that the taper slope have significant influence on the behavior and strength of columns.

References

[1] Head, M. C. and Aristizabel-Ochoa, J. D. : Analysis of Prismatic and Linearly Tapered Reinforced Concrete Columns, J. Struct. Eng., ASCE, Vol.112, No.3, pp.575-589, 1987.

[2] Richard Liew, J. Y., Shanmugam, N. E., and Lee, S. L. : Tapered Box Columns under Biaxial Loading, J. Struct. Eng., ASCE, Vol.115, No.7, pp.1697-1709, 1989.

[3] Shugyo, M. : A New Plastic Hinge Method for Steel Space Frames, Theoretical and Applied Mechanics, Vol.36, pp.245-262, 1988.

[4] Armen, H. Jr., Isakson, G., and Pifko, A.: Discrete Element Method for the Plastic Analysis of Structures subjected to Cyclic Loading, Int. Jour. Numerical Method in Engineering, Vol.2, pp.189-206, 1970.

[5] Chen, W. F. and Atsuta, T. : Theory of Beam-Columns, Vol.2, McGraw-Hill, 1977.

[6] Yoshida, Y., Masuda, N., Morimoto, T., and Hirosawa, N. : An Incremental Formulation for Computer Analysis of Space Framed Structures, Proc. JSCE, No.300, pp.21-31, 1980.